**Proceedings of the ASME 2011 Internal Combustion Engine Division Fall Technical Conference**
**ICEF2011**
**October 2-5, 2011, Morgantown, West Virginia, USA**

# ICEF2011-60030

# EQUILIBRIUM CHEMISTRY CALCULATIONS FOR ASSESSMENT OF $NO_X$ ABATEMENT STRATEGIES IN IC ENGINES

**S. M. Aithal**
Mathematics and Computer Science Division
Argonne National Laboratory
Argonne, IL 60439, USA

## ABSTRACT

*Nitrogen Enriched Air (NEA) has shown great potential in $NO_x$ reduction without the drawbacks of exhaust gas recirculation (EGR). Use of NEA in stationary natural gas engines has shown up to 70% $NO_x$ reduction with a modest 2% nitrogen enrichment. However, nitrogen enrichment beyond a point leads to degradation in engine performance in terms of power density, brake thermal efficiency and unburned hydrocarbons. Optimizing the nitrogen enrichment levels to reduce $NO_x$ without performance degradation of the engine would greatly benefit the advancement of the air separation membrane technology. Development of fast and robust modeling tools to compute the temporal variation of the in-cylinder engine pressure, temperature and $NO_x$ formation can aid experimental efforts in determining the optimum enrichment levels for a given engine operating condition. This work presents a methodology to compute engine-out $NO_x$ for engines with and without nitrogen enrichment. Temporal variation of in-cylinder engine pressure and temperature can be obtained by a solution of the energy equation. Using these temperature and pressure values, along with the instantaneous composition of the working fluid, one can evaluate the equilibrium concentration of the combustion products. Since the $NO_x$ formation freezes a few crank angle degrees after the completion of combustion, it is instructive to examine whether the equilibrium computation can provide a reasonable estimate of engine-out $NO_x$. To this end, engine-out $NO_x$ computed by using the above-mentioned procedure was obtained as a function of equivalence ratio for cases with nitrogen enrichment of 2% and no nitrogen enrichment. The results showed that the equilibrium $NO_x$ concentrations a few crank angle degrees after end of combustion were close to those reported experimentally in stationary natural gas engines. These results suggest that it would be possible to use equilibrium chemistry computations to evaluate various $NO_x$ mitigation strategies.*

## NOMENCLATURE

| | |
|---|---|
| A | surface area of cylinder head ($m^2$) |
| $a_{n,k}$ | coefficients fits to thermodynamic data of $k^{th}$ species |
| $C_{p,k}$ | molar heat capacity at constant pressure of the $k^{th}$ species (J/mole-K) |
| $C_{v,k}$ | molar heat capacity at constant volume of the $k^{th}$ species (J/mole-K) |
| $\overline{C}_p$ | mixture-averaged molar specific heat at constant pressure (J/mole-K) |
| $\overline{C}_v$ | mixture-averaged molar specific heat at constant volume (J/mole-K) |
| $G_k$ | molar Gibbs free energy of the $k^{th}$ species (J/mole) |
| $h_{cg}$ | convective heat transfer coefficient W $m^{-2}$ K |
| $H_k$ | molar enthalpy of the $k^{th}$ species (J/mole) |
| $H_P$ | enthalpy of the products (J) |
| $H_R$ | enthalpy of the reactants (J) |
| $m$ | instantaneous mass in the engine cylinder (kg) |
| $m_f$ | mass of fuel (kg) |
| $N_{rpm}$ | rotational speed of the engine (rev/min) |
| P | pressure ($N/m^2$) |
| $P_1$ | pressure at BDC |
| $Q_{in}$ | heat input from fuel combustion (J) |
| $Q_{loss}$ | heat lost from engine cylinder (J) |
| $R_g$ | gas constant (J/kg-K) |
| $R_u$ | universal gas constant (J/K) |
| $S_k$ | molar entropy of the $k^{th}$ species (J/mole-K) |
| $T(\theta)$ | average cylinder temp at crank angle $\theta$ (K) |
| $T_w$ | wall temperature (K) |
| $U_k$ | molar internal energy of the $k^{th}$ species (J/mole) |
| $V(\theta)$ | instantaneous volume at crank angle $\theta$ |
| $x_1(\theta)$ | distance of cylinder head from TDC at $\theta$ |

| | |
|---|---|
| $X_k$ | mole fraction of the $k^{th}$ species |

## GREEK SYMBOLS

| | |
|---|---|
| $\gamma$ | ratio of specific heats |
| $\theta$ | crank angle |
| $\phi$ | equivalence ratio |
| $\omega$ | engine speed (= $6N_{rpm}$ deg/sec) |

## ABBREVIATION

| | |
|---|---|
| ATDC | after top dead center |
| BDC | bottom dead center |
| EGR | exhaust gas recirculation |
| EOC | end of combustion |
| EVO | exhaust valve open |
| LHV | lower heating value |
| SI | spark ignition |
| SOI | start of injections |
| TDC | top dead center |

## 1 INTRODUCTION

Combustion processes in the transportation, utility, and industrial sectors are major sources of $NO_x$ production. $NO_x$ emissions contribute to a variety of environmental problems such as acid rain and acidification of aquatic systems, and smog. The amount of $NO_x$ formed depends on several parameters such as combustion temperature, equivalence ratio, turbulence and mixing of the fuel-air mixture, and the residence time of the combusting gases in the combustion chamber. Understanding the role of these factors in the overall $NO_x$ formation process plays an important role in developing $NO_x$ mitigation techniques. Such techniques can be broadly classified into two categories: combustion modification and post-combustion processes. The principle of combustion modification involves changing the $NO_x$ formation chemistry either by varying the reaction rates of elementary processes through temperature or by changing the concentrations of nitrogen and oxygen in the reacting zone. Use of exhaust gas recirculation (EGR) is a popular combustion modification technique to reduce $NO_x$ in automotive engines [1]. Use of EGR lowers the peak combustion temperature and also reduces the overall oxygen content in the initial charge, thus leading to reduced $NO_x$ formation. However, the use of EGR has some detrimental effects on the overall performance of the engine, such as reduction of engine power output, increased soot, and possibly unstable combustion at low loads. Nitrogen-enriched air is another technique that has shown promising results in $NO_x$ reduction in stationary natural gas engines [2].

Modeling and simulation can play an important role in engine design, analyses, and optimization studies. Complex multi-dimensional, multizone simulations (e.g., [3-5] and references therein) can elucidate the effects of important parameters such as fuel composition, engine geometry and operating conditions on fluid-dynamic variables such as temperature, pressure, velocities, and species concentrations in a variety of engines. Such complex models can also include detailed chemical kinetics to describe fuel combustion and formation of soot/UHC/$NO_x$. For instance, hydrocarbon combustion has been studied with hundreds of reactions and species ([6] and references therein). Similarly, a complex reaction mechanism for $NO_x$ formation suggested by Miller and Bowman [7] has about 51 species and over 200 reactions. Several researchers have used the KIVA family of codes—KIVA (1985), KIVA-II (1989), KIVA3 (1993), KIVA-3V (1997), and KIVA-3V Release 2 (1999—to conduct multidimensional engine simulations [8-10].

Conducting a transient multidimensional numerical simulation of the entire engine cycle consisting of intake, compression, power, and exhaust strokes is a daunting computational task. Such simulations can take several hours to days, depending on the complexity of the flow and/or chemistry model and the size of the computational domain. Hence, the required computational effort precludes its use in early stages of design, development, and assessment of $NO_x$ reduction techniques. Robust, computationally efficient, physics-based, quasi-dimensional modeling tools, on the other hand, require meager computational resources and the computational time is usually on the order of seconds. Development of such quasi-dimensional modeling tools can greatly aid the design, analyses, and optimization of a variety of $NO_x$ mitigation techniques. Such design tools can also be used for comparing the efficacy of various $NO_x$ reduction techniques. Experimental studies are useful in validating and calibrating numerical models [11-14]. These numerical models in turn can be used to examine a range of operating conditions (cylinder pressure, RPM, compression ratio, equivalence ratio) and other emission-reducing technologies (catalysts, EGR, etc.), thus complementing experimental efforts. Temporal variation of $NO_x$ during an engine cycle can be computed by using finite-rate or equilibrium chemistry computations and has been used in various quasi-dimensional models [15-16]. Both techniques have their advantages and disadvantages. Equilibrium chemistry computations depend only on the temperature, pressure, and initial elemental mixture composition (initial number of atoms of C, H, O, and N in most combustion systems). A set of about 20 species is usually adequate to describe the combustion products in most fuel-air combustion systems. Moreover, equilibrium $NO_x$ concentrations are not very sensitive to the initial concentration of trace species such as atomic nitrogen and oxygen. However, the equilibrium approach can be inaccurate in predicting the temporal variation of $NO_x$ under normal engine operating conditions. is the reason is that equilibrium computations assume that the elementary processes in $NO_x$ formation are infinitely fast compared with the residence time of the reacting mixture for a given set of conditions (temperature, pressure and composition). During the

 

compression and expansion cycle, the engine cylinder volume (and hence species concentration), pressure, and temperature are rapidly varying and are comparable to the time-constants of the reactions producing NO. This is especially true during the early phase of combustion when the cylinder temperature is not high or during the expansion stroke in the late phases of combustion. Hence the use of the equilibrium approach can lead to inaccurate prediction of the temporal thermal NO concentration [17].

Finite-rate chemistry calculations do not make any assumptions about the chemistry time-scales and hence do not have the drawbacks of the equilibrium method. However, finite-rate chemistry calculations require the use of an appropriate mechanism (set of elementary reactions and their associated reaction rate constants) to describe the $NO_x$ formation process with reasonable accuracy. Careful attention must be paid to the size of the time-step and initial conditions of trace species such as atomic nitrogen and oxygen) to ensure the stability and accuracy of the time-marching process. Finite-rate chemistry computations using an implicit variable time-stepping scheme and a reduced chemistry mechanism for $NO_x$ can be fast and robust [15]. However, one would require a more detailed reaction mechanism to describe the 20 species used in the current work. This would increase the computational time considerably. Inclusion of elementary reactions to describe fuel pyrolysis would place stringent constraints on the size of the time steps, further increasing the computational time. While the knowledge of temporal variation of $NO_x$ computed from finite-rate kinetics can provide useful information on the $NO_x$ formation process from a kinetics standpoint, for most engine designs the overall engine-out $NO_x$ is of greater interest. Equilibrium chemistry computations may thus be suitable for evaluating engine-out $NO_x$. Given these considerations, the finite-rate chemistry method was not used in the present work.

Equilibrium chemistry concentrations can be obtained by using the Gibbs free energy method, look-up tables or equilibrium constant method. The Gibbs free energy methods and look-up tables can be computationally expensive [16], whereas computations conducted by using the equilibrium constant method can be extremely fast and robust [18]. Additionally, for most combustion problems of interest to engineering applications, the equilibrium constant method is easier to formulate and implement. More important, the method can be easily coupled to quasi-dimensional codes to obtain equilibrium concentration of various species during the compression and expansion strokes. The computational time is also about an order of magnitude lower than that of the minimization of Gibbs Free energy method [18]. Given these considerations, the equilibrium constant method was chosen for this work.

In this work, we investigate the use of the equilibrium chemistry computations using the equilibrium constant method to compute the engine-out $NO_x$ and compare the results with experimental data. Since the $NO_x$ formation is believed to freeze a few crank angle degrees after the combustion process is complete, it would be instructive to compare the equilibrium $NO_x$ concentration from EOC to EVO with experimental data to assess the applicability of equilibrium methods for $NO_x$ predictions. One could also compare the relative effects of nitrogen enrichment on equilibrium $NO_x$ concentration. Based on the accuracy of the equilibrium calculations, one could evaluate the use of equilibrium chemistry computations for comparing the relative merits of NEA with other $NO_x$ reduction techniques such as EGR.

## 2 MATHEMATICAL FORMULATION

The numerical model used to study the compression and power stoke of a single-cylinder diesel engine, along with validation, is described in detail in [19]. A similar methodology was used in this work to model a spark-ignited large bore natural gas engine. Briefly, a zero-dimensional (also called quasi-dimensional) model was used to compute temporal variation of the temperature and pressure fields during the compression and power strokes. Temporal variation of the engine pressure and temperature during the compression and power stroke can be obtained by a numerical solution of the energy equation. Effects of temperature and mixture composition on the thermophysical properties of the working fluid were included in the solution of the energy equation. Temporal variations of the thermophysical properties of all the species in the gas mixture were obtained by using thermodynamic coefficients from the CHEMKIN database. Fuel combustion chemistry was modeled by a single-step global reaction. The combustion process was modeled by using the well-known Wiebe function to express the mass fraction burned. A single-zone model was used in this work since equilibrium $NO_x$ computations after EOC were of interest.[1] Equilibrium $NO_x$ was computed at each crank angle, knowing the temperature and pressure obtained from the solution of the energy equation. The basic equations solved are given below.

*Energy Equation:*

$$\frac{dP(\theta)}{d\theta} = \frac{\gamma - 1}{V(\theta)}(Q_{in} - Q_{loss}) - \gamma \frac{P(\theta)}{V(\theta)}\frac{dV}{d\theta} \quad (1)$$

$$Q_{in}(\theta) = (H_P(T) - H_R(T)) \cong m_f(\theta) LHV \quad (2)$$

$$Q_{loss}(\theta) = \frac{h_{cg} A}{\omega}(T(\theta) - T_w) \quad (3)$$

The instantaneous values of volume, area, and displacement are given by the slider-crank model [19].

$$V(\theta) = V_c + \frac{\pi D^2}{4} x_1(\theta) \quad (4)$$

[1] After EOC, the burned gas temperature equals the average cylinder temperature.

$$A(\theta) = 2\left(\frac{\pi D^2}{4}\right) + \pi D\, x_1(\theta) \tag{5}$$

$$x_1(\theta) = (l + R) - \left[R\cos\theta + \sqrt{\left(l^2 - R^2 \sin^2\theta\right)}\right] \tag{6}$$

The convective heat transfer coefficient was expressed as

$$h_{cg} = 3.26\, D^{-0.2} P^{0.8} T^{-0.55} w^{0.8} \ , \tag{7}$$

where the velocity of the burned gas $w$ is given by

$$w = c_1 S_p + c_2 \frac{V_d T_r}{p_r V_r}\left(P(\theta) - P_m\right) . \tag{8}$$

Specific heats, enthalpies, and internal energy of individual species in the working fluid were computed by using polynomials as follows.

$$\frac{C_{p,k}}{R_u} = a_{1,k} + a_{2,k}T + a_{3,k}T^2 + a_{4,k}T^3 + a_{5,k}T^4 \tag{9}$$

$$C_{v,k} = C_{p,k} - R_u \tag{10}$$

$$H_k = \left(a_{1,k} + \frac{a_{2,k}}{2}T + \frac{a_{3,k}}{3}T^2 + \frac{a_{4,k}}{4}T^3 + \frac{a_{5,k}}{5}T^4 + \frac{a_{6,k}}{T}\right)R_u T \tag{11}$$

$$U_k = H_k - R_u T \tag{12}$$

Mixture-averaged values of specific heat of the working fluid were averaged by using mole fractions as follows.

$$\overline{C}_v = \sum_{k=1}^{K} X_k C_{v,k}; \quad \overline{C}_p = \sum_{k=1}^{K} X_k C_{p,k}$$
$$\gamma = \frac{\overline{C}_p}{\overline{C}_v} \tag{13}$$

A similar procedure was used to compute the mixture-averaged values of enthalpy and internal energy of the working fluid. The Wiebe function was used to compute the burned mass fraction as shown below [20],

$$x_b(\theta) = \frac{m_{fb}}{m_{fT}} = \left\{1 - \exp\left\{-a\left(\frac{\theta - \theta_0}{\theta_b}\right)^{m+1}\right\}\right\} \ , \tag{14}$$

where $\theta$, $\theta_0$, and $\theta_b$ are the instantaneous crank angle, the crank angle for the start of combustion, and the combustion duration, respectively. Further, $m_{fb}$ is the fuel burned, and $m_{fT}$ is the total fuel at BDC. $x_b(\theta) - x_b(\theta - 1)$ is the mass of fuel burned in each crank angle and is used to compute $Q_{in}$ in Eq. (2).

The average gas temperature was obtained as

$$T(\theta) = \frac{P(\theta)V(\theta)}{m(\theta)R_g} \ . \tag{15}$$

## 3 METHOD OF SOLUTION

The numerical model described above was used to compute the average pressure and temperature in a single-cylinder natural gas engine described in [2]. Methane ($CH_4$) is used as a surrogate for natural gas in all simulations for the sake of simplicity. The procedure to obtain the cylinder pressure in a diesel engine is explained in detail in [19]. The same procedure is adapted to obtain the pressure and temperature in an SI engine using the equations described above. Briefly, for a given set of operating conditions, namely, the prescribed the mass of the fuel-air mixture and temperature at BDC, Eq. (1) was solved iteratively by using (2) through (14) to obtain the pressure from -179°<θ<180°, in increments of 1°. The corresponding temperature was obtained by using Eq. (15).

The engine dimensions and operating conditions used in this work were the same as those described in [2]. Table 1 shows the engine dimensions used in this work, and Table 2 shows the operating conditions.

Table 1: Engine dimensions

| | |
|---|---|
| Bore (mm) | 130 |
| Stroke (mm) | 140 |
| Compression ratio | 11:1 |
| Length of connecting rod (mm) | 260 |

Table 2: Operating conditions used in this work

| | |
|---|---|
| Speed (rpm) | 1800 |
| Power (kW) | 33 |
| Fuel mass (gm) | 0.13 |
| Air mass (gm) | Depends on equivalence ratio |
| Spark timing | From Ref [2] |

The mass of fuel (natural gas in this case) was kept constant at 0.13 gm for all cases. The mass of air used for the various cases is shown in Table 3. The mass of air for NEA = 0 and NEA = 2% for each value of equivalence ratio (ϕ) is the same.

Table 3: Mass of air for various equivalence ratios (mass oaf air for NEA = 0 and 2% for ϕ is the same)

| ϕ | NEA = 0% and 2% (gm) |
|---|---|
| 0.9 | 2.48 |
| 0.8 | 2.80 |
| 0.7 | 3.2 |
| 0.65 | 3.4 |

The 2% nitrogen-enriched case was simulated by assuming $O_2$:$N_2$ ratio of 1:4.15, while NEA = 0 cases had $O_2$:$N_2$ ratio of 1:3.76. A Weibe function with a = -4 and m = 2 was used in all simulations to describe the rate of fuel combustion (see Eq. (14)). The combustion duration ($\theta_b$) used in Eq. (14) was chosen such that the peak pressure matched those reported in [2] and occurred at CAD 10° ATDC in all case studies (with and without nitrogen enrichment). Ignition timing reported in [2] was used for simulations for various equivalence ratios for both NEA = 0 and NEA = 2% cases. Knowing the temporal variation of temperature, pressure, and initial elemental

composition of N, O, C, and H, (based on fuel-air composition) one can obtain the temporal variation of equilibrium concentration of a given set of combustion product species as described in [18]. In this work, the following 19 species were considered in computing equilibrium concentrations: $CH_4$, $O_2$, $CO_2$, $H_2O$, $N_2$, N, O, NO, OH, H, $N_2O$, CO, $H_2$, $NO_2$, $HO_2$, $CH_3$, $C_2H_2$, C, and HCN. These species (except the fuel, which is methane in this case) represent the most important products found in a wide range of combustion systems including automotive engines and hence were chosen for this work. Four linear equations describing the atom balances for C, H, O, and N along with 15 nonlinear equations describing the relationship between the mole fraction and equilibrium rate constants as discussed in [18] were solved with the Newton-Raphson method to obtain equilibrium concentration of all the 19 species in the system.

## 4 Results and Discussion

This section briefly discusses validation of the Newton-Raphson solver used for computing the equilibrium composition of the fuel-air mixture. Also presented are predictions of the quasi-dimensional model used to compute the temporal variation of temperature and pressure. Additionally, temporal variations of equilibrium concentrations of important species are presented. The impact of NEA on the equilibrium $NO_x$ concentrations is discussed. As an illustration, equilibrium $NO_x$ concentrations obtained by using EGR is compared with the equilibrium $NO_x$ predictions with and without nitrogen enrichment.

### 4.1 Verification of the Newton-Raphson Equilibrium Chemistry Solver

Reference [18] describes several validation cases designed to verify the accuracy and robustness of the Newton-Raphson solver used to compute equilibrium concentrations of combustion systems. A variety of fuel-additive air mixtures at various temperatures and pressures were used to rigorously test the solver. In this work, the Newton-Raphson solver was used to compute equilibrium concentration at each crank angle in the compression and expansion stroke. Temperature and pressure computed by using Eq. (1) and Eq. (15), along with the initial charge concentration (based on a given initial fuel-air mixture), were used as inputs to the solver, as explained in Section 3. Equilibrium computations were conducted for equivalence ratios 0.9 to 0.65 (with and without NEA) as reported in Ref. [2]. For the purposes of validation in this work, a single representative value of temperature, pressure (from the expansion cycle), and initial concentration as shown in Table 4 was used. Table 4 also shows the equilibrium concentrations calculated by using the Newton-Raphson solver with prediction from [21]. One can see that the predictions of the solver used in this work are in excellent agreement with the results obtained by using [21].

Table 4: Validation (Nitrogen-enriched air)

| | |
|---|---|
| Temperature (K) | 1745 |
| Pressure (atm) | 29.11 |
| Equivalence ratio | 0.65 |
| $CH_4$ (mole fraction) | 6.4344E-02 |
| $O_2$ (mole fraction) | 1.8167E-01 |
| $N_2$ (mole fraction) | 7.5399E-01 |

| | Species | Current Study (Mole Fraction) | Ref. [10] (Mole Fraction) |
|---|---|---|---|
| 1 | $CH_4$ | 4.75E-25 | 4.65E-25 |
| 2 | $O_2$ | 5.2044E-02 | 5.2031E-02 |
| 3 | $CO_2$ | 6.4334E-02 | 6.4336E-02 |
| 4 | $H_2O$ | 1.2859E-01 | 1.2859E-01 |
| 5 | $N_2$ | 7.5304E-01 | 7.5306E-01 |
| 6 | N | 2.1597E-12 | 2.1286E-12 |
| 7 | O | 2.9989E-06 | 2.9769E-06 |
| 8 | NO | 1.7905E-03 | 1.7861E-03 |
| 9 | OH | 1.7292E-04 | 1.7211E-04 |
| 10 | H | 7.5118E-08 | 7.4355E-08 |
| 11 | $N_2O$ | 4.8862E-07 | 4.8704E-07 |
| 12 | CO | 5.9285E-06 | 5.8858E-06 |
| 13 | $H_2$ | 3.3125E-06 | 3.2893E-06 |
| 14 | $NO_2$ | 1.2838E-05 | 1.2812E-05 |
| 15 | $HO_2$ | 9.4717E-07 | 9.4297E-07 |

### 4.2 Results from the Quasi-Dimensional Model

Figure 1 shows the temporal variation of temperature for various values of equivalence ratios ($\phi$) for the case without nitrogen enrichment. It is seen that the temperature rises slowly during the compression stroke, followed by a rapid increase after SOI as a result of fuel combustion. The peak temperature occurs just after TDC and drops during the expansion cycle. Moreover, the peak cylinder temperature drops monotonically with $\phi$. Equation (15) shows that the higher the mass of the working fluid (fuel and air mass), the lower the average temperature for a given pressure. As the value of $\phi$ decreases the mass of air in the cylinder increases, (see Table 3) which leads to lower peak temperatures. For all values of $\phi$ considered in this paper, the temporal variations of temperature with and without nitrogen enrichment were almost identical (and hence not shown separately). This result is to be expected because the peak pressure, location of maximum peak pressure, power, and

initial charge (mass of fuel and air mixture) were also identical for these cases.

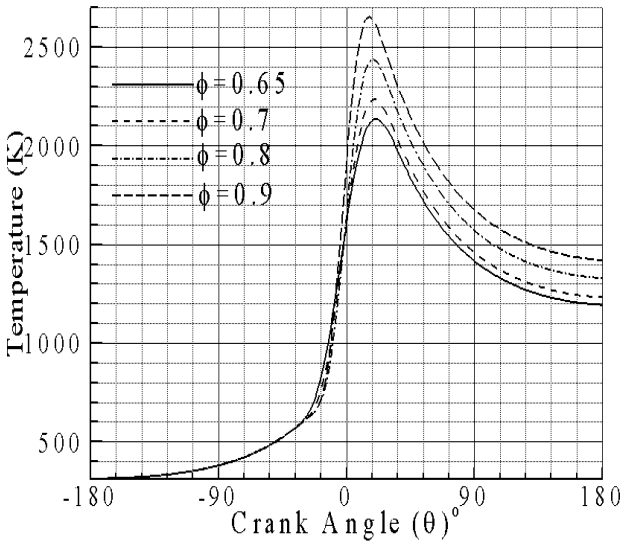


Figure 1: Temporal variation of temperature for various values of ϕ without nitrogen enrichment

Figure 2 shows the temporal variation of the mixture-averaged value of γ for ϕ = 0.9 without nitrogen enrichment.

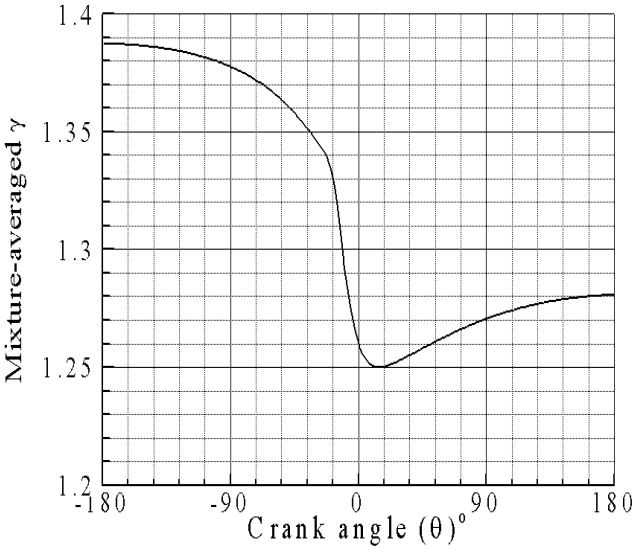


Figure 2: Temporal variation of gamma without nitrogen enrichment.

As expected, the mixture-averaged value of γ decreases continuously in the compression stroke with the increase in cylinder temperature. After SOI, there is a steep drop in γ on account of the steep rise in temperature (due to the fuel combustion) as seen in Figure 1. The cylinder temperature drops during the expansion cycle, thereby leading to an increase in γ. This behavior is seen in all the cases considered in this work.

Figure 3(a) and (b) show the temporal variation of $O_2$ and $N_2$ for ϕ = 0.8 with and without nitrogen enrichment. As expected, the mole fraction of $O_2$ in the case with nitrogen enrichment is lower than that without enrichment, while the opposite is true for $N_2$.

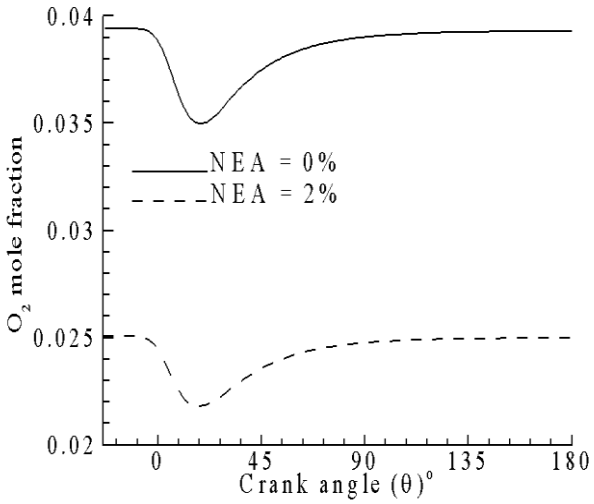


(a)

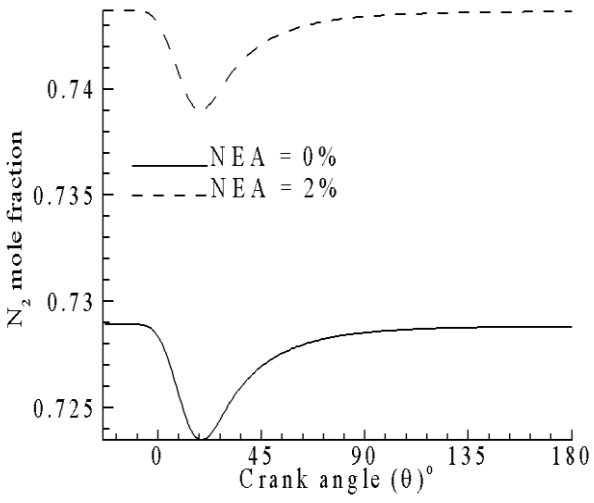


(b)

Figure 3: Temporal variation of $O_2$ (a), and $N_2$ (b).

One can also see that when the engine temperature rises, the mole fractions of $O_2$ and $N_2$ decrease from their expected values corresponding to complete combustion. This decrease continues till the engine temperature reaches its peak just after TDC. This

reduction of the equilibrium concentrations of $O_2$ and $N_2$ is due to the formation of other species such as O, N, NO, $N_2O$, and OH etc. As the temperature and pressure drop during the expansion cycle the mole fractions of both $O_2$ and $N_2$ return to the values expected from a single step complete combustion reaction for both NEA = 0 and NEA = 2% cases.

Figure 4 shows the mole fractions of O and OH as a function of crank angle for the case without nitrogen enrichment. Mole fractions of O and OH reach a peak as the engine temperature reaches its peak. One can see that the drop in the $O_2$ mole fraction is almost equal to the increase in the mole fraction of OH just after TDC where the engine temperature reaches its peak. Similar characteristics are seen for the case with nitrogen enrichment.

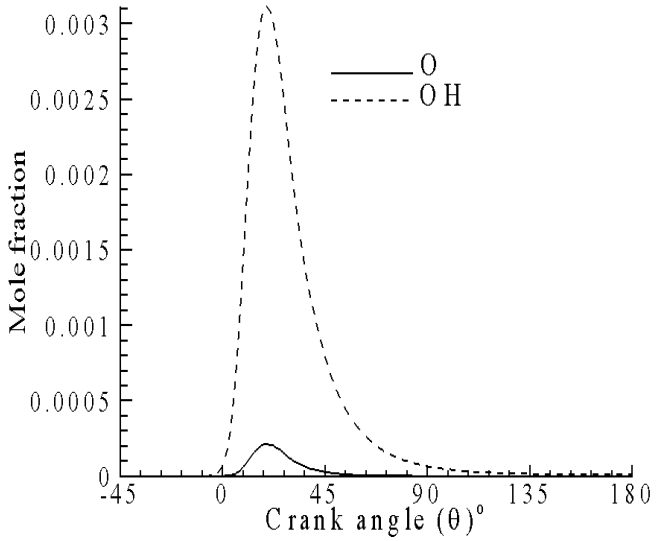


Figure 4: Mole fractions of O and OH.

Figure 5 (a) and (b) show the temporal variation of NO (in ppm) as a function of crank angle for $\phi = 0.8$ with and without nitrogen enrichment. Figure 5 (a) shows the entire cycle whereas Figure 5 (b) shows temporal variation on NO towards the end of combustion. As expected, Figure 5 (a) shows that the NO concentration reaches its maximum just after TDC, where the engine temperature and pressure reach their peak values. In an actual engine, the fuel combustion typically ends 15–25°ATDC. The rate of depletion of $O_2$ due to combustion in the engine cylinder is greatly reduced toward the end of combustion. Additionally, the average engine cylinder temperature and pressure also drop during the expansion cycle. The combined effect of these two processes freezes the NO concentration. The engine-out NO measured experimentally at EVO is thus very close to this frozen NO concentration, which occurs a few degrees after EOC. It is instructive to examine whether the NO concentrations predicted by equilibrium assumptions a few degrees after EOC are close to experimentally measured engine-out NO.

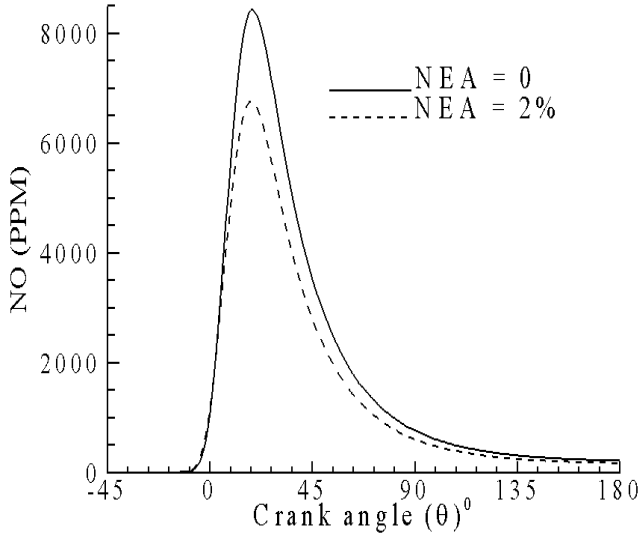


(a)

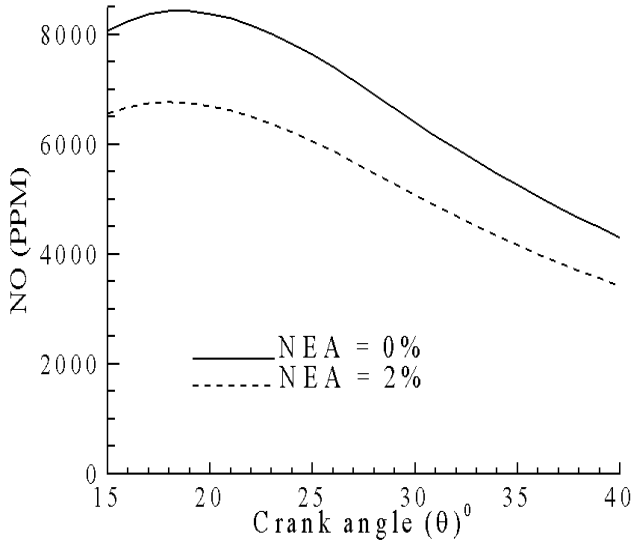


(b)

Figure 5: Temporal variation of NO (ppm) for $\phi = 0.8$ with and without nitrogen enrichment.

Figure 6 shows a comparison of experimental engine-out NO data with results from the equilibrium solver with and without nitrogen enrichment. The CAD at which the NO concentration closely matches experimental data is shown in Table 5.

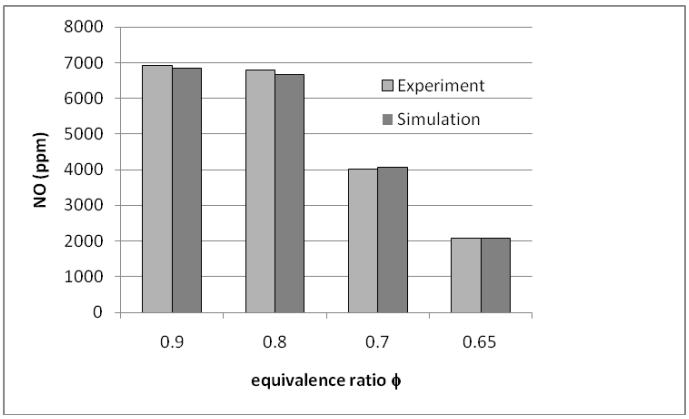


(a)

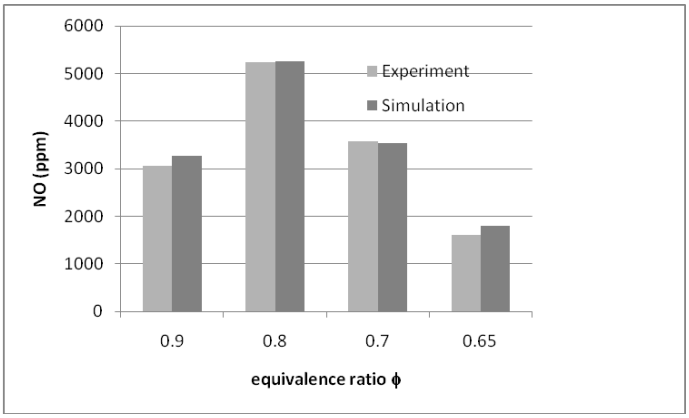


(b)

Figure 6: Comparison of experimental engine-out NO with simulations: (a) no nitrogen enrichment and (b) with nitrogen enrichment.

Table 5: CAD at which NO concentration closely matches experimental data

| ϕ | EOC (CAD) | | CAD for Reported NO | |
|---|---|---|---|---|
| | NEA = 0% | NEA = 2% | NEA = 0% | NEA = 2% |
| 0.9 | 22 | 24 | 25 | 30 |
| 0.8 | 26 | 26 | 29 | 29 |
| 0.7 | 30 | 30 | 38 | 38 |
| 0.65 | 34 | 35 | 51 | 52 |

Figure 6 (a) and (b) along with Table 5 show that the NO concentration predicted by equilibrium considerations are very close to experimentally measured values. The results also show that engine-out NO matches that predicted by equilibrium assumptions a few CAD after EOC (3 to 15 CAD in this case).

From this discussion, one can see that equilibrium chemistry computations can be used to obtain reasonable estimates of engine-out NO both with and without nitrogen enrichment. Temporal variation of NO (as shown in Figure 5) can be used to evaluate other NO abatement strategies. As an example, the use of EGR for a given value of air mass would enable a comparison between NO concentration obtained with nitrogen enrichment and with EGR. Such an evaluation was done for the $\phi = 0.8$ case.

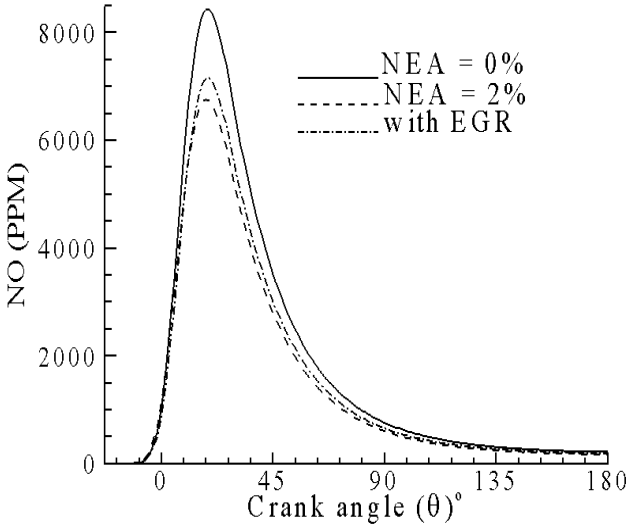


(a)

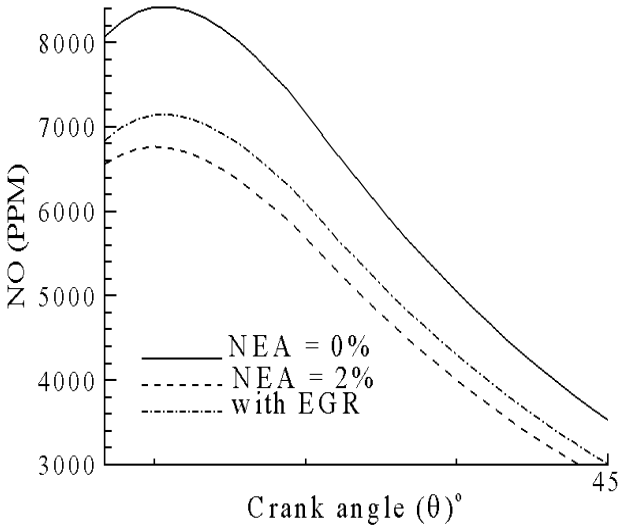


(b)

Figure 7: Comparison of NO with EGR and nitrogen enrichment.

The equivalence ratio and EGR fraction was adjusted such that the total mass of air and EGR equaled the mass of air for $\phi$ = 0.8 case (2.8 gm as shown in Table 3). This adjustment was accomplished by using $\phi$ = 0.85 and a EGR fraction of 0.06.

Figure 7 shows the temporal variation of NO with EGR along with the cases representing 0% and 2% EGR. As expected, use of EGR reduces the overall NO as compared with the case with no nitrogen-enrichment. It is also seen that the NO concentration with 2% enrichment is more effective at reducing the concentration of NO at all crank angles.

Figure 8 shows the temporal variation of the mole fractions of NO and $NO_2$. It is seen that mole fraction of $NO_2$ is about 3 orders of magnitude lower than NO, hence $NO_x$ concentration is almost entirely NO. A similar trend is seen with nitrogen enrichment.

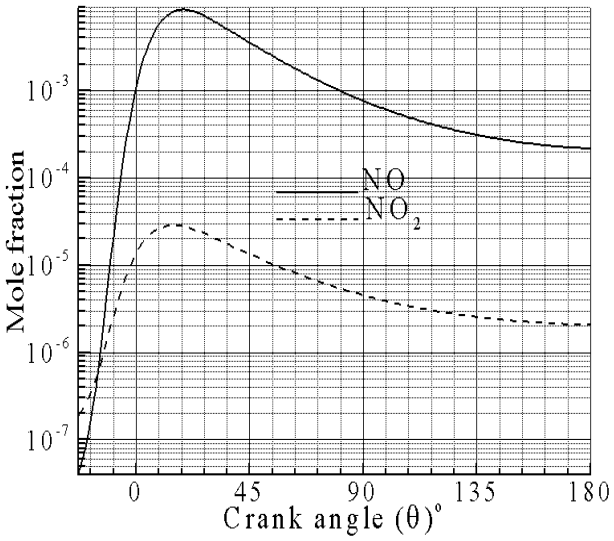


Figure 8: Comparison of NO and $NO_2$ mole fractions for $\phi$ = 0.8.

## 5 Conclusions

This work focused on evaluating the use of equilibrium chemistry computations as a method to compute engine-out $NO_x$. A quasi-dimensional model was used to compute the temporal variation of temperature and pressure in the engine. Using the mixture composition, temperature, and pressure, we computed the equilibrium composition of the combustion products using the equilibrium constant method. The results showed that the $NO_x$ concentration computed by using equilibrium chemistry closely matched the measured engine-out $NO_x$ a few degrees after EOC. Equilibrium computations also correctly predicted the trends of engine-out $NO_x$ with nitrogen enrichment. Equilibrium chemistry calculations were used to compare the efficacy of EGR and nitrogen enriched air in $NO_x$ formation. For the case studied in this work, NEA is indeed better than EGR for $NO_x$ reduction. Equilibrium concentrations of $NO_2$ were about three orders of magnitude lower than NO; hence, $NO_x$ concentration is almost fully NO in all the computations studied in this work. Based on these results, equilibrium computations can be used to obtain reasonable estimates of engine out $NO_x$. Furthermore these computations have the potential to be used to evaluate various $NO_x$ abatement strategies in engines.


### ACKNOWLEDGMENTS

This work was supported in part by the U.S. Dept. of Energy under Contract DE-AC02-06CH11357.


### REFERENCES


1. Zheng M, Reader G. T, Hawley J. G. 2004.Diesel engine exhaust gas recirculation—a review on advanced and novel concepts", Energy Conversion and Management Vol. 45, pp. 883–900
2. Biruduganti M., Gupta S., Bihari, B., McConnell S., Sekar R. Air separation membranes – an alternative to EGR in large bore natural gas engines. ASME Internal Combustion Engine 2009 Spring technical conference paper ICES2009-76054, 2009.
3. Sun Y, Reitz RD. Modeling diesel engine $NO_x$ and soot reduction with optimized two-stage combustion. SAE paper 2006-01-0027, 2006.
4. Kong SC, Reitz RD., 2002. Application of detailed chemistry and CFD for predicting direct injection HCCI engine combustion and emissions. Proceedings of the Combustion Institute. Vol. 29(1), pp. 663-669.
5. Etheridge J, Mosbach S, Kraft M, Wu H, Collings H. A Detailed Chemistry Multi-cycle Simulation of a Gasoline Fueled HCCI Engine Operated with NVO. SAE paper 2009-01-0130, 2009
6. Lindstedt RP, Maurice LQ. A detailed chemical kinetic model for aviation fuels," AIAA Paper 97-2836 Seattle, WA, July 1997.
7. Miller JA, Bowman CT. 1989. Mechanism and modeling of nitrogen chemistry in combustion. Prog. Energy Combustion Sci. Vol.15(4), 287-338.
8. Kong S, Marriott C, Reitz R, and Christensen M. Modeling and Experiments of HCCI Engine Combustion Using Detailed Chemical Kinetics with Multidimensional CFD. SAE Technical Paper 2001-01-1026, 2001.
9. Sun Y. and Reitz R. Modeling Diesel Engine NOx and Soot Reduction with Optimized Two-Stage Combustion. SAE Technical Paper 2006-01-0027, 2006.

10. Tan Z and Reitz R. 2006. An ignition and combustion model based on the level-set method for spark ignition engine multidimensional modeling Combustion and Flame. Vol 145(1,2) 1-15

11. Singh S. Reitz RD, Musculus MPB. Comparison of the characteristic time (CTC), representative interactive flamelet (RIF), and direct integration with detailed chemistry models against optical diagnostic data for multi-mode combustion in a heavy-duty DI diesel engine. SAE paper 2006-01-0055, 2006.

12. Hildenbrand F, Schulz C, Wolfrum J, Keller F and Wagner E. 2000. Laser diagnostic analysis of NO formation in a direct injection diesel engine with pump-line-nozzle and common rail injection systems. Proceedings of the Combustion Institute Vol. 28(1),pp 1137-1143.

13. Kashdan J. and Papagni J. LIF Imaging of Auto-ignition and Combustion in a Direct Injection Diesel-fuelled HCCI Engine. SAE Technical Paper 2005-01-3739

14. De Zilwa, S. and Steeper, R. Predicting NOX Emissions from HCCI Engines Using LIF Imaging. SAE Technical Paper 2006-01-0025, 2006.

15. Aithal SM., 2010. "Modeling of $NO_x$ formation in diesel engines using finite-rate chemical kinetics", Applied Energy; Vol. 87(7), pp. 2256-2265.

16. Andersson M, Johansson B, Hultqvist A, Nöhre C. A real time $NO_x$ model for conventional and partially premixed diesel combustion. SAE 2006-01-0195, 2006

17. Eggels RLGM. Modelling of combustion processes and NO formation with reduced reaction mechanisms. Ph.D. dissertation, Eindhoven University of Technology, 1995.

18. Aithal SM. Equilibrium chemistry calculations for lean and rich hydrocarbon-air mixtures. Journal of Gas turbines and Power (under review). Also Preprint ANL/MCS-P1825-0111, January 2011.

19. Aithal, S. M., 2009. Impact of EGR fraction on diesel engine performance considering heat loss and temperature-dependent properties of the working fluid. Int. J. Energy Research Vol. 33(4), pp 415–430.

20. Heywood J. B., 1988. Internal Combustion Engine Fundamentals. McGraw-Hill: New York

21. http://navier.engr.colostate.edu/tools/equil.html.